

## Quantum disproportionation: The high hydrides at elevated pressures

Kazutaka Abe<sup>1</sup> and N. W. Ashcroft<sup>2</sup><sup>1</sup>Research Institute of Electrical Communication, Tohoku University, 2-1-1 Katahira, Aoba, Sendai, Miyagi 980-8577, Japan<sup>2</sup>Laboratory of Atomic and Solid State Physics, Cornell University, Clark Hall, Ithaca, New York 14853-2501, USA

(Received 27 July 2013; published 22 November 2013)

A quartet of hydrogens can be dynamically bound to group-14 atoms, the resulting complexes having even valence. In macroscopic assemblies and at high pressures these can give way by dynamically assisted (quantum) disproportionation to complexes with odd valence and hence, in principle, to metallic tendencies. A new extended metallic composition of, for example, GeH<sub>3</sub> is investigated by first-principles methods within density functional theory. Its stoichiometry and its very existence is a direct consequence of inclusion of nuclear quantum dynamical contributions to the free energy. From enthalpic comparisons GeH<sub>3</sub> augmented with hydrogen appears preferred beyond 175 GPa, where three candidate structures are competitive, these being A15, *P4<sub>2</sub>/mmc*, and *Cccm*. The pressure at which GeH<sub>3</sub> makes its appearance is significantly influenced by zero-point energy, and quantum effects play an important role in a notable trend towards disproportionation. The ensuing systems are all metallic and the superconducting transition temperature of GeH<sub>3</sub> has been estimated as about 100 K or higher (a common range for the three prospective structures). The general proposition of quantum disproportionation at elevated pressures appears extendable to other high hydrides.

DOI: [10.1103/PhysRevB.88.174110](https://doi.org/10.1103/PhysRevB.88.174110)

PACS number(s): 74.62.Fj, 71.30.+h, 74.10.+v, 74.70.Ad

Once metallized at elevated pressures hydrogen-rich extended systems have been proposed to exhibit notably high superconducting transition temperatures ( $T_c$ ),<sup>1–3</sup> where the phonon-based pairing mechanism is suggested to be the same as that for pure metallic hydrogen itself.<sup>4</sup> Various high hydrides have been so far investigated both theoretically and experimentally.<sup>5</sup> One of the more interesting predictions from theory is that the A15 (*Pm $\bar{3}n$* ) structure can be stabilized in AlH<sub>3</sub>,<sup>6,7</sup> and also in GaH<sub>3</sub>;<sup>8</sup> the A15 phase was later confirmed for AlH<sub>3</sub> in experiment.<sup>9</sup> This A15 structure is particularly notable for its prominence in superconductivity (see, for example, Refs. 10–12). To date there are over 70 binaries which take up the A15 structure, and about 50 of them are superconductors. For AlH<sub>3</sub>, however, the A15 phase does not exhibit a high value of  $T_c$ , at least below 164 GPa.<sup>9</sup> For GaH<sub>3</sub>, on the other hand,  $T_c$  of the A15 phase is estimated theoretically to be 73 K at 160 GPa (with the Coulomb parameter  $\mu^* = 0.13$ ).<sup>8</sup> Yet  $T_c$  actually decreases with compression, being predicted to fall to 48 K at 240 GPa. The chief reason for the disparate behaviors in AlH<sub>3</sub> and GaH<sub>3</sub> is that the Fermi energy lies around the lower reaches of a pseudogap which makes the density of states (DOS) at the Fermi energy somewhat more sensitive to structural conditions. In fact, for AlH<sub>3</sub>, even a transformation into a semiconducting phase is suggested at 200 GPa.<sup>7</sup>

Given this it is of considerable interest to examine other group-14 elements and their possible combinations and stoichiometries with hydrogen, especially those neighboring Al and Ga. Since the electron number is clearly increased in proceeding to the group-14 constituents, the Fermi energy is expected to rise beyond the pseudogap, the DOS at the Fermi energy being larger and then less sensitive to structural conditions. In typical A15 compounds XTr<sub>3</sub>, where X is in many cases a group-13 or 14 element and Tr a transition-metal element, Al and Ga are very often replaceable by Si, Ge, and Sn. The trend of the occurrence of the A15 structure is especially similar for the constituents Al, Ga, and Ge,<sup>12</sup>

suggesting at least a possibility of GeH<sub>3</sub> taking up the A15 structure. Accordingly we have performed a preliminary analysis of the enthalpy of A15 XH<sub>3</sub> binaries for group-14 X, and have observed that an A15 form of GeH<sub>3</sub> is indeed quite possible at high pressures. From recent theoretical work by Gao *et al.*,<sup>13</sup> GeH<sub>4</sub> is reported to be unstable to elemental decomposition up to 220 GPa, but is then said to be restabilized beyond 220 GPa, where the structure has the *C2/c* symmetry. The associated electronic structure is metallic, and the  $T_c$  calculated from McMillan's formula is high, in fact reaching 64 K. However, conditions of high density may well change the chemical trends and, accordingly, might lead to some quite different compositions such as, we are suggesting, GeH<sub>3</sub>. Although the most kinetically persistent germanium hydride is germane, GeH<sub>4</sub>, and completely in line with standard chemical instincts, it is important to recognize that, for example, the combinations Si<sub>2</sub>H<sub>6</sub> (di-silane), Ge<sub>2</sub>H<sub>6</sub> (di-germane), and Sn<sub>2</sub>H<sub>6</sub> (di-stannane) are already known to exist in molecular forms.

Motivated in part by the above, and the potential of the A15 structure for enhanced superconductivity, we have chosen to investigate GeH<sub>3</sub> at high pressures not only in the A15 structure but also some nearby modifications. First-principles calculations are performed by using density functional theory within the generalized gradient approximation.<sup>14</sup> We use VASP,<sup>15</sup> which utilizes plane-wave basis sets and the projector augmented-wave (PAW) method.<sup>16</sup> The outermost cutoff radii of the PAW pseudopotentials are 1.01 Å for Ge (with *3d4s4p* as valence) and 0.42 Å for H (with *1s* as valence). The cutoff energy is set at 700 eV and Brillouin zone sampling is carried out with a  $k$ -point number of  $n_k \sim (40 \text{ \AA})^3/v_{\text{cell}}$ , where  $v_{\text{cell}}$  is the volume of the unit cell. A Fermi-distribution smearing is used with a temperature of  $k_B T = 0.1$  eV. For the computations of  $T_c$ , we make use of density functional perturbation theory, where QUANTUM ESPRESSO<sup>17</sup> is used. The outermost cutoff radii of the ultrasoft pseudopotentials are again 1.16 Å for Ge and 0.42 Å for H (possible sensitivity

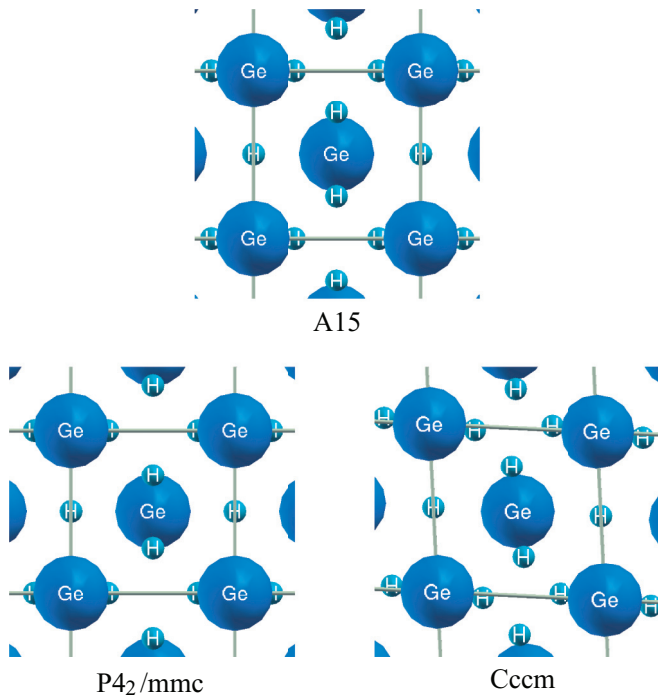


FIG. 1. (Color online) The A15, the  $P4_2/mmc$ , and the  $Cccm$  structures at  $r_s = 1.52$  ( $\sim 180$  GPa). The structural parameters of the latter two are as follows: in the  $P4_2/mmc$ ,  $a = b = 3.033$  Å,  $c = 3.318$  Å, Ge at  $2c$  sites (0.0, 0.5, 0.0), H at  $2e$  sites (0.0, 0.0, 0.25), and  $4k$  sites (0.2244, 0.5, 0.5); in the  $Cccm$ ,  $a = 4.718$  Å,  $b = 4.292$  Å,  $c = 3.014$  Å, Ge at  $4e$  sites (0.25, 0.25, 0.0), H at  $4b$  sites (0.0, 0.5, 0.25), and  $8l$  sites (0.1043, 0.8726, 0.0).

to these has been checked), and the cutoff energy is set at 612 eV. The numbers of  $k$  points and  $q$  points (the phonon wave vectors) are, respectively,  $18 \times 18 \times 18$  and  $6 \times 6 \times 6$ , at  $r_s = 1.52$ ; here  $r_s$  is defined as usual by  $[3/(4\pi n_e)]^{1/3}/a_0$ , where  $a_0$  is the Bohr radius, and  $n_e$  is the average density of valence electron (with the Ge  $3d$  electrons excluded here).

The A15 structure for  $\text{GeH}_3$  can be viewed as a simple cubic lattice with two Ge and six H atoms per primitive cell, the Ge atoms occupying body-centered-cubic sublattice sites and the H atoms, in pairs, forming three orthogonal chains (Fig. 1). In searching for nearby candidate structures, we have performed constant-pressure and also constant-temperature molecular dynamics with the A15 structure as an initial configuration. From these simulations, we have arrived at the  $Cccm$  structure, which is obtained by distorting the A15 into a base-centered-orthorhombic form. Also, we have encountered the  $P4_2/mmc$  structure by inspecting the effects of tetragonal distortion on the A15.<sup>10</sup> There are two  $P4_2/mmc$  structures; one is with  $c/a > 1$  and the other is with  $c/a < 1$ . Here, we focus our discussion on the first with  $c/a > 1$  because it has lower enthalpy than the second (even with the harmonic zero-point energy considered). In fact, neither the  $Cccm$  nor the  $P4_2/mmc$  structures are far removed from the A15 structure as shown in Fig. 1. Moderate pairing of H atoms accompanies the distortion in both the structures, and this pairing is even more prominent in the  $P4_2/mmc$  structure.

The enthalpy of these structures is presented in Fig. 2, where it is given for the composite system ( $\text{GeH}_3 + \text{H}$ ) in

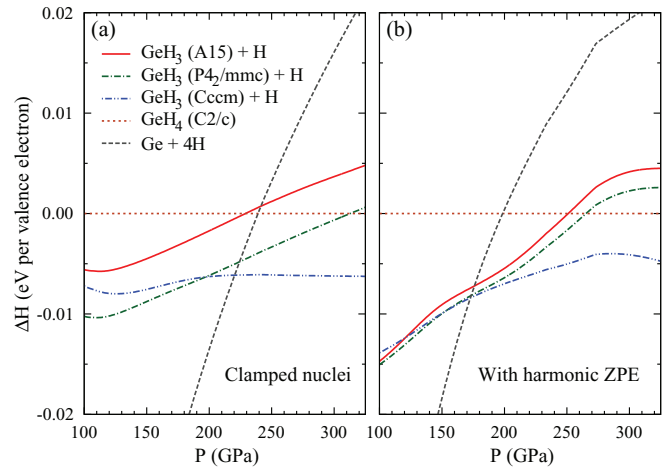


FIG. 2. (Color online) The enthalpy of  $\text{GeH}_4$ ,  $\text{GeH}_3 + \text{H}$ , and  $\text{Ge} + 4\text{H}$  systems: (a) in the clamped nuclei approximation; (b) in the harmonic approximation for the zero-point energy. The C2/c structure (Ref. 13) of  $\text{GeH}_4$  is taken as a reference. The enthalpy of elemental Ge is calculated for the  $Cmca$  (Refs. 18 and 19) and hcp structures (Ref. 20), and that of elemental H is for the C2/c (Ref. 21), the  $Cmca$ -12 (Ref. 21), the  $Cmca$  (Ref. 22), and the Cs-IV ( $I4_1/amd$ ) (Ref. 23) structures.

order to make a direct comparison with that of  $\text{GeH}_4$ . The enthalpy of the system with complete elemental decomposition ( $\text{Ge} + 4\text{H}$ ) is also shown. While Fig. 2(a) gives the results within the clamped nuclei approximation, Fig. 2(b) presents them with the zero-point energy included, this within the harmonic approximation. The zero-point energy is calculated by applying the frozen-phonon method with the Phonopy algorithm.<sup>24</sup> We have used a  $2 \times 2 \times 2$  supercell containing 64 atoms regarding  $\text{GeH}_3$ , and the resulting zero-point energies of the A15, the  $P4_2/mmc$ , and the  $Cccm$  structures at, for example, 180 GPa are 0.1058, 0.1096, and 0.1085 eV per valence electron, respectively. Whether the zero-point energy is included or not,  $\text{GeH}_3$  remains a possibility at high pressure, and it tends to take the  $Cccm$  structure as pressure is increased. Yet, there exist two quite prominent effects of the zero-point energy. One is that the transition pressure from  $\text{Ge} + 4\text{H}$  into  $\text{GeH}_3 + \text{H}$  is considerably lowered, from 220 to 175 GPa. Thus, in this pressure range the pathway of the disproportionation is significantly affected by the quantum effects of nuclei (hence the very suggestion of quantum disproportionation). The other is that with the zero-point energy incorporated, the A15 structure becomes very competitive with the  $P4_2/mmc$  and the  $Cccm$  structures around the transition pressure. Put in other terms, zero-point energy seems to favor more isotropic structures. As a matter of fact, a similar tendency was previously predicted for solid hydrogen itself,<sup>25</sup> where anharmonicity is also included through the self-consistent harmonic approximation. If the anharmonic effects, which are not taken into account in Fig. 2(b), further favor isotropic structure, there then remains a possibility that the A15 structure will appear around 175 GPa where the three structures are quite competitive.

Figure 3 shows the DOS per valence electron and the partial DOS (PDOS) of the A15, the  $P4_2/mmc$ , and the  $Cccm$  structures, together with those of the A15  $\text{GeH}_3$  for

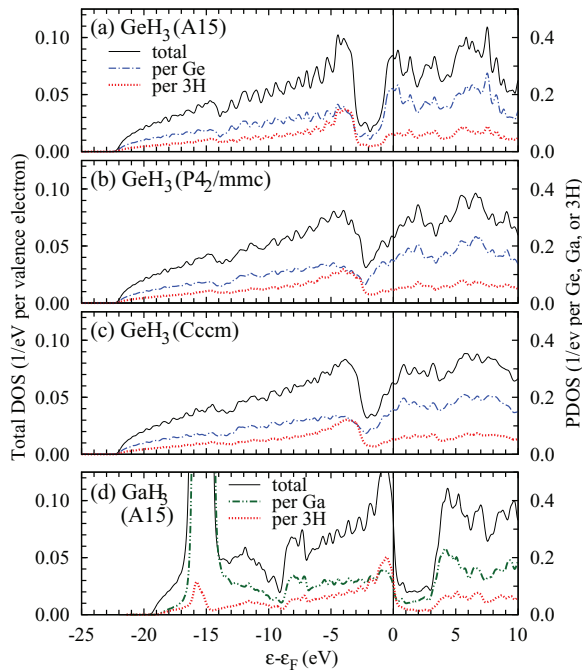


FIG. 3. (Color online) The DOS and the PDOS of  $\text{GeH}_3$  at  $r_s = 1.52$  ( $\sim 180$  GPa), where those of  $\text{GaH}_3$  at  $r_s = 1.58$  ( $\sim 180$  GPa) are also shown for comparison: (a) the A15 ( $Pm\bar{3}n$ )  $\text{GeH}_3$ ; (b) the  $P4_2/mmc$   $\text{GeH}_3$ ; (c) the  $Cccm$   $\text{GeH}_3$ ; (d) the A15  $\text{GaH}_3$ . The DOS at the Fermi energy of  $\text{GeH}_3$  is close to the free electron value  $3/(2\epsilon_F)$ , which is now  $\sim 0.068 \text{ eV}^{-1}$  with  $\epsilon_F$  set to  $22 \text{ eV}$ .

comparison. As noted, with the replacement of Ga by Ge, the Fermi energy is raised and lies above the pseudogap. In order to achieve credible superconductivity, it is necessary to have a high DOS at the Fermi energy. For a reasonably free electron system, the DOS per electron at the Fermi energy  $\epsilon_F$  is  $3/(2\epsilon_F)$ , and for all three structures of  $\text{GeH}_3$  the DOS at the Fermi energy is indeed quite comparable to this value. In particular, in the A15 structure, the Fermi energy lies on a peak just above the pseudogap, so that rather high values of the DOS at the Fermi energy are actually brought about. In the PDOS at the Fermi energy, the contribution from the H atoms can be seen. Thus, the electronic states near the Fermi energy overlap very well with the protons and, therefore, are expected to couple strongly to high frequency phonons, which is another key factor for achieving potentially high  $T_c$  values.

In Fig. 4, we present the density of phonon modes as well as the Eliashberg spectral function multiplied by  $2/\omega$ , the latter being the integrand of the electron-phonon coupling parameter  $\lambda (\equiv \int d\omega 2\alpha^2 F/\omega)$ , and also the weight function required for obtaining  $\langle \log \omega \rangle (= \log \omega_{\log})$ . The phonon modes beyond  $400 \text{ cm}^{-1}$  are essentially traceable to hydrogen motion, and those below  $400 \text{ cm}^{-1}$  to germanium motion. There are no imaginary phonon frequencies in the three structures around this pressure and they are therefore mechanically stable with respect to any subsequent atomic motion (with cell fixed) originating with the clamped nuclei picture. The highest phonon frequency is about  $1800 \text{ cm}^{-1}$ , which is somewhat lower than that found for the  $C2/c$  structure of  $\text{GeH}_4$  (about  $2600 \text{ cm}^{-1}$  at  $220 \text{ GPa}$ ).<sup>13</sup> The high frequency in the  $C2/c$   $\text{GeH}_4$  can be traced to the proton pairs with a

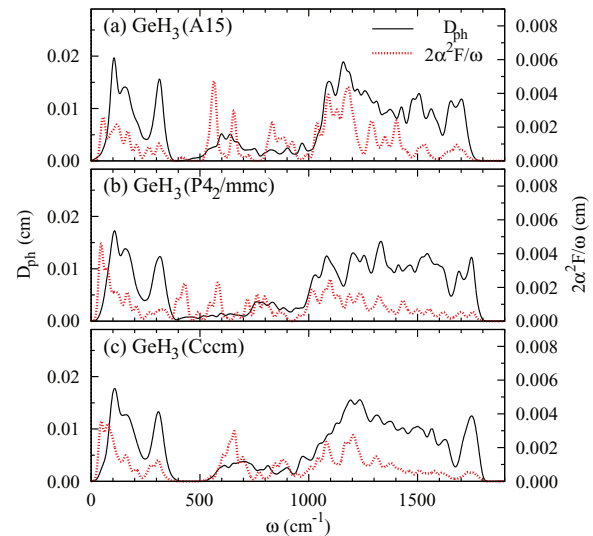


FIG. 4. (Color online) The densities of phonon modes  $D_{\text{ph}}$  and the integrand of  $\lambda$  (i.e.,  $2\alpha^2 F/\omega$ ) of  $\text{GeH}_3$  at  $r_s = 1.52$  ( $\sim 180$  GPa): (a) the A15 ( $Pm\bar{3}n$ ) structure; (b) the  $P4_2/mmc$  structure; (c) the  $Cccm$  structure. The resulting  $\lambda$  and  $\omega_{\log}$  are, respectively, 1.82 and  $989 \text{ K}$  in the A15 structure, 1.56 and  $737 \text{ K}$  in the  $P4_2/mmc$  structure, and 1.60 and  $793 \text{ K}$  in the  $Cccm$  structure.

corresponding average separation of  $0.87 \text{ \AA}$ . The A15 form of  $\text{GeH}_3$ , as well as nearby arrangements, do not have quite such tightly identifiable pairs. The lower phonon frequencies in  $\text{GeH}_3$  might be seen as a possible disadvantage for attaining high  $T_c$ , but the electron-phonon coupling turns out to be a considerable compensating advantage. Indeed, the  $2\alpha^2 F/\omega$  remains appreciable at high frequencies despite the factor  $1/\omega$ , and both  $\lambda$  and  $\omega_{\log}$  are accordingly large as described in the caption to Fig. 4. (For comparison purposes,  $\lambda$  is 1.12 and  $\omega_{\log}$  is  $897 \text{ K}$  in the  $C2/c$   $\text{GeH}_4$  at  $220 \text{ GPa}$ .<sup>13</sup>) The notable manifestation of strong electron-phonon coupling in  $\text{GeH}_3$  is largely attributable to the high DOS at the Fermi energy. The  $T_c$  is estimated from the McMillan formula<sup>26</sup> along with the Allen-Dynes corrections,<sup>27</sup> and is shown in Fig. 5 as a function of  $\mu^*$ . At  $\mu^* = 0.13$ , which is generally considered reasonable for typical metals, the  $T_c$  at  $180 \text{ GPa}$  is  $140 \text{ K}$  in the A15

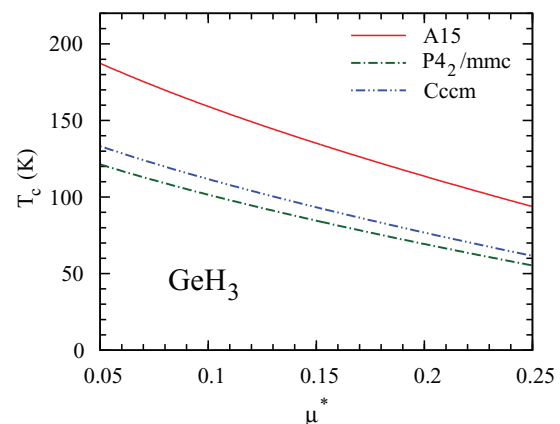


FIG. 5. (Color online) The  $T_c$  of  $\text{GeH}_3$  at  $r_s = 1.52$  ( $\sim 180$  GPa) as a function of  $\mu^*$ . The  $T_c$  is calculated from the McMillan equation with the Allen-Dynes corrections.

structure, 90 K in the  $P4_2/mmc$  structure, and 100 K in the  $Cccm$  structure.

The electronic structures of the hydrogen-based A15 compounds  $XH_3$  (i.e.,  $AlH_3$ ,  $GaH_3$ , and  $GeH_3$ ) are somewhat different from those of well-known A15 compounds  $XTr_3$  with Tr taken as a typical transition metal. For  $XTr_3$  there are generally very flat and isotropic bands around the  $\Gamma$  point near the Fermi energy, which are thought to influence both the martensitic transition and superconductivity.<sup>10</sup> By contrast, there exists a clear direct band gap at the  $\Gamma$  point in the  $XH_3$ . Another difference is that, while a significant bonding is observed along Tr chains in the  $XTr_3$ , such a bonding is not found in H chains of the  $XH_3$ . This is natural because the effective atomic size of H is very small compared with those of transition metal Tr. Instead, for example, in  $GeH_3$ , prominent charge accumulation is observed between H and Ge atoms. This charge distribution is similar to that in  $GaH_3$  as expected from the PDOS (Fig. 3), though less ionic when compared with that in  $AlH_3$ .<sup>7</sup>

An intriguing feature possibly common to both  $XH_3$  and  $XTr_3$  classes is that the Fermi energy is controllable to some extent through the choice of the constituent elements and their stoichiometries. As noted above, the number of valence electrons in  $XH_3$  has a notable influence on the DOS at the Fermi energy and, consequently, on  $T_c$ . This is also the case in  $XTr_3$ . Indeed, the  $XTr_3$  systems with high  $T_c$ 's (beyond 10 K) have essentially a common number of valence electrons per atom (about 4.6),<sup>10–12</sup> and such high- $T_c$  substances also have Fermi energies located at peaks of the DOS. Whether  $X$  belongs to group 13 or group 14 does not drastically change the DOS at the Fermi energy in metallic  $XTr_3$ . This follows because the DOS is already large owing to the defining presence of  $d$  states of the transition metal Tr. In some contrast to this, in metallic  $XH_3$ , the position of the Fermi energy is sensitive to the valence of  $X$  because H only possesses a single  $s$  state and the DOS is small. Notice that the DOS of  $GeH_3$  does not possess any substantial dip above the Fermi energy in the A15,  $P4_2/mmc$ , or  $Cccm$  structures. Thus, it would also be interesting to investigate

$XH_3$  with group-15 choices for  $X$ , for the DOS at the Fermi energy is expected to remain high. As an example,  $SbH_3$  might well be a candidate since Sb is sometimes replaceable by Al, Ga, and Ge in typical A15 compounds.

By way of summary, a trihydride of germanium has been investigated at high pressures using density functional theory. When zero-point energies are taken into account within the harmonic approximation this  $GeH_3$  stoichiometry becomes stable beyond 175 GPa, where the nearby competing structures are A15 ( $Pm\bar{3}n$ ),  $P4_2/mmc$ , and  $Cccm$ . The zero-point energy has two prominent effects. One is that it lowers the pressure of the transition into  $GeH_3$  by about 45 GPa, crucially affecting the subsequent pathway of disproportionation. The other is that it favors the isotropic A15 structure. The ensuing metallicity of these structures leads on to a study of possible superconductivity, and the transition temperature  $T_c$  is estimated to exceed 100 K at 180 GPa. In particular, the  $T_c$  of the A15 structure is high and reaches 140 K. Although the A15 structure is not the most stable within the harmonic approximation, there remains an uncertainty stemming from anharmonicity since the energy differences among the three structures are fairly small around 175 GPa. If anharmonic effects further favor isotropic structures (a matter now under investigation), the stabilization of the A15 structure and quite high  $T_c$ 's appear likely. Though we have concentrated here on the germanium/hydrogen system the arguments given have some generality indicating that if, through choice of constituents and their densities the zero-point energies acquire large values the concept of quantum disproportionation could be applicable to a range of systems.

This work was supported in part by the National Science Foundation under Grant No. DMR 130 3598 and by a Grant-in-Aid for Scientific Research from the MEXT under Grant No. 25400353. K.A. gratefully acknowledges the support from the Mayekawa Houonkai Foundation. We are especially grateful to Professor Roald Hoffmann and his group for stimulating discussions on hydride systems.

<sup>1</sup>J. J. Gilman, *Phys. Rev. Lett.* **26**, 546 (1971).

<sup>2</sup>N. W. Ashcroft, *J. Phys.: Condens. Matter* **16**, S945 (2004).

<sup>3</sup>N. W. Ashcroft, *Phys. Rev. Lett.* **92**, 187002 (2004).

<sup>4</sup>N. W. Ashcroft, *Phys. Rev. Lett.* **21**, 1748 (1968).

<sup>5</sup>See, for example, T. A. Strobel, A. F. Goncharov, C. T. Seagle, Z. Liu, M. Somayazulu, V. V. Struzhkin, and R. J. Hemley, *Phys. Rev. B* **83**, 144102 (2011); P. Zaleski-Ejgierd, R. Hoffmann, and N. W. Ashcroft, *Phys. Rev. Lett.* **107**, 037002 (2011).

<sup>6</sup>C. J. Pickard and R. J. Needs, *Phys. Rev. B* **76**, 144114 (2007).

<sup>7</sup>M. Geshi and T. Fukazawa, *Physica B* **411**, 154 (2013).

<sup>8</sup>G. Gao, H. Wang, A. Bergara, Y. Li, G. Liu, and Y. Ma, *Phys. Rev. B* **84**, 064118 (2011).

<sup>9</sup>I. Goncharenko, M. I. Erements, M. Hanfland, J. S. Tse, M. Amboage, Y. Yao, and I. A. Trojan, *Phys. Rev. Lett.* **100**, 045504 (2008).

<sup>10</sup>M. Kataoka and N. Toyota, *Phase Transitions* **8**, 157 (1987).

<sup>11</sup>J. Muller, *Rep. Prog. Phys.* **43**, 641 (1980).

<sup>12</sup>D. Dew-Hughes, *Cryogenics* **15**, 435 (1975).

<sup>13</sup>G. Gao, A. R. Oganov, A. Bergara, M. Martinez-Canales, T. Cui, T. Iitaka, Y. Ma, and G. Zou, *Phys. Rev. Lett.* **101**, 107002 (2008).

<sup>14</sup>J. P. Perdew, in *Electronic Structure of Solids '91*, edited by P. Ziesche and H. Eschrig (Akademie Verlag, Berlin, 1991), p. 11; J. P. Perdew, K. Burke, and M. Ernzerhof, *Phys. Rev. Lett.* **77**, 3865 (1996).

<sup>15</sup>G. Kresse and J. Hafner, *Phys. Rev. B* **47**, R558 (1993); **49**, 14251 (1994); G. Kresse and J. Furthmüller, *Comput. Mater. Sci.* **6**, 15 (1996); *Phys. Rev. B* **54**, 11169 (1996).

<sup>16</sup>P. E. Blöchl, *Phys. Rev. B* **50**, 17953 (1994); G. Kresse and D. Joubert, *ibid.* **59**, 1758 (1999).

<sup>17</sup>P. Giannozzi *et al.*, *J. Phys.: Condens. Matter* **21**, 395502 (2009).

<sup>18</sup>F. J. Ribeiro and M. L. Cohen, *Phys. Rev. B* **62**, 11388 (2000).

<sup>19</sup>K. Takemura, U. Schwarz, K. Syassen, M. Hanfland, N. E. Christensen, D. L. Novikov, and I. Loa, *Phys. Rev. B* **62**, R10603 (2000).

<sup>20</sup>Y. K. Vohra, K. E. Brister, S. Desgreniers, A. L. Ruoff, K. J. Chang, and M. L. Cohen, *Phys. Rev. Lett.* **56**, 1944 (1986).

<sup>21</sup>C. J. Pickard and R. J. Needs, *Nat. Phys.* **3**, 473 (2007).

<sup>22</sup>B. Edwards, N. W. Ashcroft, and T. Lenosky, *Europhys. Lett.* **34**, 519 (1996).

<sup>23</sup>K. Nagao, H. Nagara, and S. Matsubara, *Phys. Rev. B* **56**, 2295 (1997).

<sup>24</sup>Atsushi Togo, Fumiyasu Oba, and Isao Tanaka, *Phys. Rev. B* **78**, 134106 (2008).

<sup>25</sup>D. M. Straus and N. W. Ashcroft, *Phys. Rev. Lett.* **38**, 415 (1977).

<sup>26</sup>W. L. McMillan, *Phys. Rev.* **167**, 331 (1968).

<sup>27</sup>P. B. Allen and R. C. Dynes, *Phys. Rev. B* **12**, 905 (1975).